A Numerical Investigation of the Effect of Increasing Blade Numbers on Cavitation and Performance of Centrifugal Pumps at Constant Parameters

Hayder Kareem Sakran

lecturer, Chemical Engineering Department /University of Muthanna

E-mail: haider_skran@yahoo.com

Abstract

In the present paper, a numerical study has been investigated by using computational fluid dynamics (CFD) to analyze pressure, head, head coefficient, pressure coefficient, input power, and volume fraction of cavitation at three cases of simulation in which each one has constant parameters; however, with modifying number of blades which is changed from five to sixteen.

The constant parameters are rotating speed, volume flow rate, mass flow rate, outlet diameter, suction specific speed N_{ss}, Reynolds number and NPSHr. These parameters have been fixed to have the same conditions for each case. The shear stress transport (SST) turbulence model has been used to inspect a steady state incompressible flow through centrifugal pump numerically. The simulation has done by using ANSYS$^®$, Vista CPD^{TM} Release 15.0. The results are plotted and discussed to describe and find a relation among cavitation, pump behavior, and variation of blade numbers at constant conditions. The results show a strong relation among increasing blade numbers, centrifugal pump performance and reducing pump cavitation.

Keywords- ANSYS$^®$, Vista CPD^{TM} Release 15.0, Cavitation, Centrifugal pump, CFD, Number of blades, Numerical Simulation.

تحري عددي لتاثير زيادة عدد ريش البشارة على ظاهرة التكهف و اداء المضخات النابذة تحت عوامل ثابتة

م. حيدر كريم سكران

كلية الهندسة/جامعة المثنى

haider_skran@yahoo.com

الخلاصة

في هذا البحث تم اجراء دراسة عددية باستعمال ديناميكيا الموائع الحسابية (CFD) لتحليل الضغط و الارتفاع و معامل الضغط و معامل الارتفاع و القدرة الداخلة و التكهف لثلاث حالات من المحاكات. تم محاكاة كل حالة تحت عوامل ثابتة مع الاخذ بنظر الاعتبار تعديل عدد ريش البشارة و التي تم زيادتها من خمسة الى ست عشرة .

شملت العوامل الثابتة سرعة الدوران و معدل الجريان الحجمي و معد الجريان الكتلي و القطر الخارجي و سرعة الامتصاص النوعية N_{ss} و رقم رينولد و NPSHr . تم تثبيت هذه المعملات للحصول على ظروف متشابهة لكل حالة. و تم استعمال المعامل الاضطرابي (SST) لفحص الجريان بحالتة المستقرة و الغير انضغاطية عدديا خلال المضخات النابذة. و تم اجراء المحاكاة باستعمال برنامج (ANSYS$^®$, Vista CPD^{TM} Release 15.0). تمت مناقشة النتائج لوصف وايجاد العلاقة بين التكهف و سلوك المضخة و عدد الريش تحت ظروف ثابتة. و اظهرت النتائج علاقة قوية بين زيادة عدد ريش البشارة و اداء المضخة الانتباذية و تقليل التكهف.

الكلمات المفتاحية : التكهف، المضخة الانتباذية، عدد ريش البشارة ، دراسة عددية ، ديناميكيا الموائع الحسابية.

1. INTRODUCTION

Centrifugal pump can be found all around at several places, used in different locations, especially in industrial and other sectors such as agriculture, domestic applications …etc. The main goal of using centrifugal pump is to transfer fluid between two places by rotating impeller. Moreover, it is used to raise fluid pressure and fluid kinetic energy which has been done by supplying fluid with mechanical energy that is done by transferring energy from electric motor to centrifugal pump by rotating shaft. [1], [2]. However, design and prediction of centrifugal pump performance are very hard to be covered since it needs a complex three-dimensional computational domain to simulate fluid flow through it.

Impeller rotating causes increasing liquid velocity around it and makes it higher than the liquid that either entering or leaving the pump; therefore, pressure on the rotating part will be in its lower case because velocity increases. Whereas flow velocity is high, pressure is low and vice versa, [3]. [4]. In addition, placing a small amount of liquid in a closed system also can reduce pressure of liquid, then a certain part of liquid will vaporize. Vaporization indicates that equilibrium happens between molecule leaving and incoming of liquid. Pressure that exerted vaporization during the phase of equilibrium is known as a vapor pressure, which is related to the phase of changing liquid. [5], [6].

Since molecular energy is a function of temperature, vapor pressure increases with temperature increasing. For example, for water at zero ^{o}C vapor pressure will be zero Pa, and it is 1 atmosphere 101.235 kpa when temperature is 100 ^{o}C. [3]. Table 1 shows variations of vapor pressure of water at different temperatures. When vapor pressure increases higher than the absolute pressure at any point of centrifugal pump, vapor bubble or cavitation bubble will be generated and swept away from low-pressure region then collapsed. This phenomenon is known as cavitation. [7]

Cavitation is a phenomenon that should be avoided or minimized since it causes a lot of pump problems such as erosion, generating annoying, vibration, surface pitting, fatigue failure, flow rate reduction, and reducing equipment performance and efficiency. [8]. All of these problems push designer to consider cavitation during equipment production. Avoiding cavitation is an extremely important situation and it can be achieved by increasing liquid pressure everywhere inside the pump more than vapor pressure. To enhance that a parameter calls Net Positive Section Head NPSH has been employed for monitoring cavitation. A lot of investigations have been employed to study cavitation and its effect on pumps performance.

Cavitation can be generated in place where leading edge meets tip. Cavitation zone will move from leading edge to trailing edge when NPSH value is minimized. Additionally, when cavity

length reaches its maximum chord length of a blade, NPSH curve will be dropped [9]. To avoid cavitation, the required and available NPSH should be equalized [10]. Cavitation can also be minimized if pump works with low head. [11]. Some parameters such as head value, flow rate, and pumps efficiency remain constant with reducing NPSH available. [12] At a specific NPSH decreasing, head value remains constant. [11]. However, with further NPSH available reducing, these parameters are reduced. At 3% of head drop, flow rate will be reduced to 2% and pump efficiency will also be decreased to 3%. [13] During cavitation, pressure of vanes passes decreases because of the existence of vapor bubbles in liquid and that can decrease the fullness of dynamic pressure measurement of the specific frequency.

Table1. Saturation (Vapor) pressure of water at various temperatures [3]

Temperature $^{\circ}$C	Saturation pressure Kpa	Temperature $^{\circ}$C	Saturation pressure Kpa
-10	0.26	30	4.25
-5	0.403	40	7.38
0	0.611	50	12.35
5	0.872	100	101.3(1 atm)
10	1.23	150	475.8
15	1.71	200	1554
20	2.34	250	3973
25	3.17	300	8581

 Examining variation of blade numbers either experimentally or numerically to study their effects on centrifugal pump performance and pump cavitation at a rotating part- pump impeller-has not been satisfied, since few of researchers discuss this field.

Flow domain through impeller is extremely complicated. In addition, it depends upon blade numbers. [14]. Flow domain can be controlled strongly with increasing number of blades since increasing blade numbers will increase blockage and that will generate a big ratio between the solid and the liquid inside flow field [15]. Increment of impeller blade numbers has a strong influence on the design of the relative flow angle at trailing edge of a blade as shown in figure 1 [15]. Centrifugal pump design can be controlled by blade numbers depending on fluid type. The impeller used to deliver liquid will have a smaller number of blades than the one that is used to deliver gas, because liquid impeller should have thicker blades than the gas impeller [16].
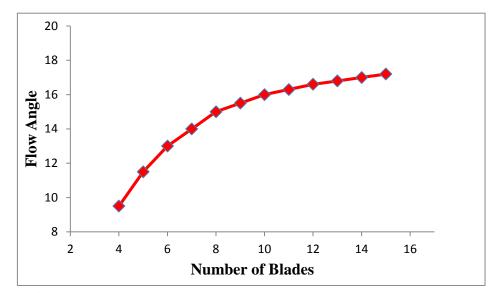
Figure 1. The relation between flow angle and number of blades. [15]

This paper investigates variation of blade numbers in centrifugal pump and examines pump cavitation at pressure drop region using computational fluid dynamic which is applied by a commercial software ANSYS®, Vista CPD^TM Release 15.0. The results give a respectable understanding that can engage to develop centrifugal pump with reducing or preventing cavitation.

2. NUMERICAL ANALYSIS AND MATHEMATICAL MODEL

Analysis of flow attitude inside computational domain of centrifugal pump is extremely complicated because the three-dimensional flow structure has a turbulence, cavitation, and mixture flow. [17]

Since thirty years ago, computational fluid dynamics has been employed to understand the computational domain of turbomachinery problems and other turbulence equations. It has a huge application for researchers to carry out a lot of investigations to tackle centrifugal pump. Available commercial CFD code, ANSYS®, Vista CPD^TM Release 15.0 has been used to simulate the three-dimensional turbulence flow that passes through geometry of centrifugal domain. The governing equation has been solved and analyzed numerically by CFD using Shear Stress Transport (SST) as a turbulence model. [18]. Computational fluid dynamics gives a wealthy vision to flow condition and helps to enhance opulent information about turbulence flow behavior inside turbomachinery equipment.

 In the centrifugal pump, there is a flow of the mixture of liquid, its vapor, and noncondensable gas, which is steady, three-dimensional, turbulent, and isothermal. The continuity equation, momentum equations, and Shear-Stress Transport (SST) k- ω Model for the mixture of liquid, vapor, and noncondensable gas are provided in Ref. [19], [20] and [21].

The description of the three dimensional model for centrifugal pump and incompressible mixture flow can be expressed with the laws of the conservation of mass and conservation of momentum with a cylindrical coordinate.

The continuity equation for the mixture model can be expressed as:

$$\frac{\partial}{\partial t}(\rho_m) + \nabla.(\rho_m \vec{v}_m) = 0 \tag{1}$$

Where $\vec{v}_m$ is the mass-averaged velocity:

$$\vec{v}_m = \frac{\sum_{k=1}^{n} \alpha_k \rho_k \vec{v}_k}{\rho_m} \tag{2}$$

ρ_m is the mixture density:

$$\rho_m = \sum_{k=1}^{n} \alpha_k \rho_k \tag{3}$$

α_k is the volume fraction of phase k.

We can achieve the momentum equation for the mixture by summing the individual momentum equation for all phases. It can be shown as:

$$\frac{\partial}{\partial t}(\rho_m \vec{v}_m) + \nabla(\rho_m \vec{v}_m \vec{v}_m) = -\nabla p + \nabla.\left[\mu_m(\nabla \vec{v}_m + \nabla \vec{v}_m^T)\right] + \rho_m \vec{g} + \vec{F} + \nabla.\left[\sum_{k=1}^{n} \alpha_k \rho_k \vec{v}_{dr,k} \vec{v}_{dr,k}\right]$$

(4)

Where n is the number of phases, F is the body force, and µ is the viscosity of the mixture:

$$\mu_m = \sum_{k=1}^{n} \alpha_k \mu_k \tag{5}$$

$\vec{v}_{dr,k}$ is the drift velocity for secondary phase k:

$$\vec{v}_{dr,k} = \vec{v}_k - \vec{v}_m \tag{6}$$

From the continuity equation for secondary phase p, the following volume fraction equation for secondary phase p can be obtained:

$$\frac{\partial}{\partial t}(\alpha_p \rho_p) + \nabla.(\alpha_p \rho_p \vec{v}_m) = -\nabla.(\alpha_p \rho_p \vec{v}_{dr,p}) + \sum_{q=1}^{n}(\dot{m}_{qp} - \dot{m}_{pq}) \tag{7}$$

where $\dot{m}_{qp}$ is the mass transfer from phase q to phase p and $\dot{m}_{pq}$ is the mass transfer from phase p to phase q.

During the simulation, the turbulence model chosen was the Shear-Stress Transport (SST) k- ω Model because of its stability. This model was used to resolve partial differential equations for

turbulent kinetic energy and the dissipation rate as shown by the Equations below. The SST k-ω model has a similar form to the standard k-ω model. [21]

$$\frac{\partial}{\partial t}(\rho k)+\frac{\partial}{\partial x_i}(\rho k u_i)=\frac{\partial}{\partial x_i}\left(\Gamma_k\frac{\partial k}{\partial x_i}\right)+\tilde{G}_k-Y_k+S_k \tag{8}$$

and

$$\frac{\partial}{\partial t}(\rho \omega)+\frac{\partial}{\partial x_j}(\rho \omega u_j)=\frac{\partial}{\partial x_j}\left(\Gamma_\omega\frac{\partial \omega}{\partial x_j}\right)+G_\omega-Y_\omega+D_\omega+S_\omega \tag{9}$$

All terms of the SST k-ω model are explained below:
  I.   The effective diffusivities for the SST k-ω model are given by:

$$\Gamma_k=\mu+\frac{\mu_t}{\sigma_k} \qquad \Gamma_\omega=\mu+\frac{\mu_t}{\sigma_\omega}$$

Where σ_k and σ_ω are the turbulent Prandtl numbers for k and ω, respectively.

$$\sigma_k=\frac{1}{F_1/\sigma_{k,1}+(1-F_1)/\sigma_{k,2}} \tag{10}$$

$$\sigma_\omega=\frac{1}{F_1/\sigma_{\omega,1}+(1-F_1)/\sigma_{\omega,2}} \tag{11}$$

The turbulent viscosity, μ_t , is calculated as follows:

$$\mu_t=\frac{\rho k}{\omega}\frac{1}{\max\left[\frac{1}{\alpha^*},\frac{SF_2}{a_1\omega}\right]} \tag{12}$$

The coefficient α^* damps the turbulent viscosity causing a low-Reynolds number correction.

$$\alpha^*=\alpha^*_\infty\left(\frac{\alpha^*_0+R_{et}/R_k}{1+R_{et}/R_k}\right) \tag{13}$$

Where:

$$R_{et}=\frac{\rho k}{\mu\omega} \quad , \ R_k=6, \ \alpha^*_0=\frac{\beta_i}{3} \ , \quad \beta_i=0.072$$

$$F_1=\tanh(\phi_1^4) \tag{14}$$

$$\phi_1=\min\left[\max\left(\frac{\sqrt{k}}{0.09\omega y},\frac{500\mu}{\rho y^2\omega}\right),\frac{4\rho k}{\sigma_{\omega,2}D_\omega^+ y^2}\right] \tag{15}$$

$$D_\omega^+=\max\left[2\rho\frac{1}{\sigma_{\omega,2}}\frac{1}{\omega}\frac{\partial k}{\partial x_j}\frac{\partial \omega}{\partial x_j},10^{-10}\right] \tag{16}$$

$$\phi_2 = \max\left[2\frac{\sqrt{k}}{0.09\omega y}, \frac{500\mu}{\rho y^2 \omega}\right] \tag{17}$$

$$F_2 = \tanh(\phi_2^2) \tag{18}$$

Where y is the distance to the next surface and D_ω^+ is the positive portion of the cross-diffusion term.

II.   We can express the production of turbulence kinetic energy $\tilde{G}_k$ as:

$$\tilde{G}_k = \min(G_k, 10\rho\beta^* k\omega) \tag{19}$$

The G_k term represents production of turbulence kinetic energy

$$G_k = \mu_t S^2 \tag{20}$$

Where S is the modulus of the mean rate-of-strain tensor, defined as:

$$S \equiv \sqrt{2S_{ij}S_{ij}} \tag{21}$$

$$\beta^* = \beta_i^*\left[1 + \zeta^* F(\mu_t)\right] \tag{22}$$

$$\beta_i^* = \beta_\infty^*\left(\frac{4/15 + (R_{et}/R_\beta)^4}{1 + (R_{et}/R_\beta)^4}\right) \tag{23}$$

Where $\zeta^* = 1.5$, $R_\beta = 8$, $\beta_\infty^* = 0.09$

III.   The G_ω term represents the production of ω:

$$G_\omega = \frac{\alpha}{V_t}\tilde{G}_k \tag{24}$$

IV.   The term Y_k represents dissipation of turbulence kinetic energy.

$$Y_k = \rho\beta^* k\omega \tag{25}$$

V.   The term Y_ω represents dissipation of ω.

$$Y_\omega = \rho\beta\omega^2 \tag{26}$$

$$\beta = \beta_i\left[1 - \frac{\beta_i^*}{\beta_i}\zeta^* F(\mu_t)\right] \tag{27}$$

VI.   The term D_ω represents cross-diffusion:

$$D_\omega = 2(1 - F_1)\rho\frac{1}{\omega\sigma_{\omega,2}}\frac{\partial k}{\partial x_j}\frac{\partial \omega}{\partial x_j} \tag{28}$$

The model constants are:

$\sigma_{k,1} = 1.176$, $\sigma_{\omega,1} = 2$, $\sigma_{k,2} = 1.0$, $\sigma_{\omega,2} = 1.186$, $\alpha_1 = 0.31$, $\beta_{i,1} = 0.076$, $\beta_{i,2} = 0.0828$

Some parameters such as suction specific speed, head coefficient and capacity coefficient which can be calculated from equations (29), (30), and (31) were fixed in this work as shown in table 2. [3]

$$N_{SS} = \frac{\omega Q^{\bullet 1/2}}{NPSHr^{3/4}} \tag{29}$$

$$C_H = \frac{gH}{\omega^2 D^2} \tag{30}$$

$$C_Q = \frac{Q^{\bullet}}{\omega D^3} \tag{31}$$

where

N_{SS} = Suction Specific Speed

C_H = Head Coefficient

C_Q = Capacity Coefficient

ω = pump shaft rotational speed (rpm)

$Q^{\bullet}$ = flow rate capacity (m^3/s)

3. BOUNDARY CONDITIONS AND MESH GENERATION

A steady state condition and incompressible fluid flow have been simulated through a centrifugal pump with three cases; each one has specific parameters and all parameters for each individual case are constant regardless blade numbers, since blade numbers will be variable and they will be from five to sixteen and this helps to have more conception about the effect of blade numbers on pump performance. Cavitation also has been carried out with two-phase flow (i.e., water and vapor) at 25 ^{o}C and saturation pressure with 3170 Pa.

The explanation of computational domain and boundary condition has been summarized in table 2. Moreover, mesh information is exposed in tables 3, 4 and 5.

Table 2. Summary of input, performance, and boundary conditions for cases 1, 2 and 3.

Boundary Conditions	Case 1	Case 2	Case 3	Units
Rotation Speed	366.519	397.935	418.879	[radian s^-1]
Mass Flow Rate	15	18	20	[kg s^-1]
Volume Flow Rate	0.015	0.018	0.02	[m^3 s^-1]
Inlet Total Pressure	101325	101325	101325	[Pa]
Ref. Diameter	0.1285	0.1262	0.1247	[m]
Ref. Tip Speed	23.5472	25.1087	26.1222	[m s^-1]
Ref. Density	999.808	999.844	1000.06	[kg m^-3]
Ref. Flow Coefficient	0.0386	0.045	0.0492	
Ref. Reynolds Number	167140000	175040000	179980000	
Capacity Coefficient	0.0193	0.0225	0.0246	
Machine Type	Centrifugal Pump	Centrifugal Pump	Centrifugal Pump	
Suction specific speed, N_{ss}	3.15	3.15	3.15	
Turbulence Model	Shear Stress Transport (SST)	Shear Stress Transport (SST)	Shear Stress Transport (SST)	
Fluid	Water at Standard Conditions	Water at Standard Conditions	Water at Standard Conditions	
Analysis Type	Steady State	Steady State	Steady State	
Inflow/Outflow Boundary Template	Mass Flow Inlet/P-Static Outlet	Mass Flow Inlet/P-Static Outlet	Mass Flow Inlet/P-Static Outlet	
NPSHr	4.53	3.59	5.2	[m]

To increase accuracy of computational results and to converge cavitation simulation, unstructured hybrid mesh, i.e. tetrahedra mesh with hexahedra core, is generated. Moreover, to ensure mesh size independence, a fine mesh has been employed for flow domain as shown in figure (2), and details of meshes are shown in tables 4, 5 and 6 for the three cases.
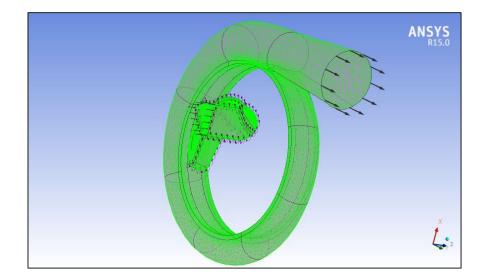
Figure 2. Mesh generation. [22]

Table 3. Mesh information for case 1. [22]

Mesh Information for Case 1					
Number of Blades	Number of Nodes	Number of Elements	Tetrahedra	Wedges	Hexahedra
5	367398	469893	112413	76200	281280
6	363598	466441	113426	76535	276480
7	354798	454506	111006	75120	268380
8	356224	453857	110052	73535	270270
9	361226	457934	110334	74060	273540
10	369962	466693	110978	74195	281520
11	361596	457613	110328	73775	273510
12	364925	460081	109666	73695	276720
13	360636	457641	111431	74680	271530
14	366627	461938	109833	74725	277380
15	363976	460588	110483	76175	273930
16	350109	448723	112398	76195	260130

Table 4. Mesh information for case 2. [22]

Mesh Information for Case 2					
Number of Blades	Number of Nodes	Number of Elements	Tetrahedra	Wedges	Hexahedra
5	365550	471726	115871	77395	278460
6	367587	472590	116325	76755	279510
7	362937	466370	114765	76385	275220
8	366906	467909	114654	74885	278370
9	369760	468773	113378	74295	281100
10	374023	473264	113939	74805	284520
11	365776	465047	114162	74705	276180
12	372905	473366	115551	75455	282360
13	365156	465599	115334	75615	274650
14	365644	465959	114784	76525	274650
15	364781	467194	116879	77165	273150
16	361670	462714	115889	76645	270180

Table 5. Mesh information for case 3. [22]

Mesh Information for Case3					
Number of Blades	Number of Nodes	Number of Elements	Tetrahedra	Wedges	Hexahedra
5	366511	473422	117242	76460	279720
6	360896	467498	117953	76395	273150
7	365220	470358	116888	76510	276960
8	355241	460021	116946	75775	267300
9	374953	476653	116478	75265	284910
10	366545	467410	115645	74775	276990
11	368864	469997	116027	75150	278820
12	363307	465224	116634	75740	272850
13	365181	466948	116568	75940	274440
14	362604	465607	117067	77550	270990
15	355524	457851	116691	76470	264690
16	362179	464683	117513	76690	270480

4. RESULTS AND DISCUSSION

Cavitating flows in a centrifugal pump were examined by using CFD method and a cavitation model when centrifugal pump transports water. A few new techniques, such as tetrahedral mesh with core hexahedral cells technique, were investigated to ensure the numerical computational procedure whether it is stable and accurate.

A good agreement has been achieved between minimizing pump cavitation and improving pump performance with increasing impeller blades. Rise pressure increases with increasing blade numbers. Since increasing number of blades can reduce flow velocity so that (where is the subject) will increase pressure "Pressure is low at locations where the flow velocity is high, and pressure is high at locations where the flow velocity is low". This is shown in figure (3). Increasing pressure has a very important effect on improving pump performance since increasing pressure will increase head rise of pump as shown in figure (4). In additions, head coefficient is increased step by step until it gets large with increment which can be clearly realized in figure (5). In consequence, pump performance is improved with all of these increments as shown in figure (6).

With increasing pressure, minimizing cavitation can be reached because fluid pressure will be higher than the absolute pressure then cavitation bubble will or will not be created with fewer amounts than with less number of blades as shown in figure (7). Figures (8), (9) and (10) show a comparison of vapor contours of cavitation at different blade numbers.

Any improvement can have disadvantages; thus, improving pump performance with minimizing cavitation has a disadvantage which is using more power input than the impeller with less number of blades. Therefore, that needs more electricity, to enhance that means more cost, which is an eligible choice to be carried with. Figure (11) shows the disadvantage of increasing blade numbers.
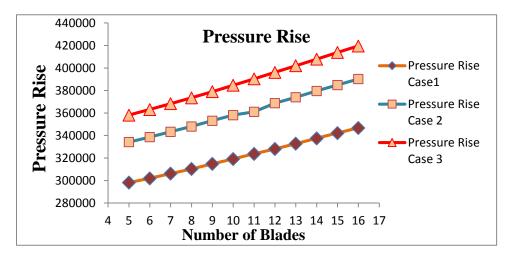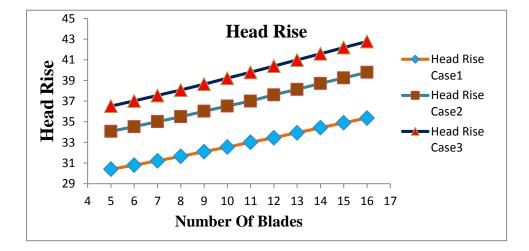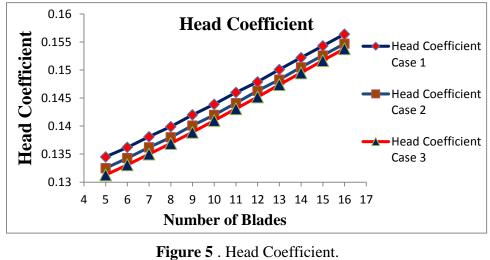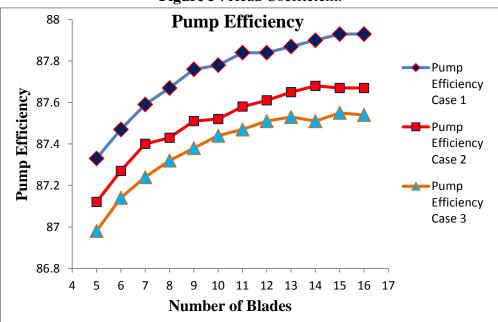

Figure 3 . Pressure Rise.

Figure 4 . Head Rise.

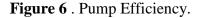
Figure 5 . Head Coefficient.

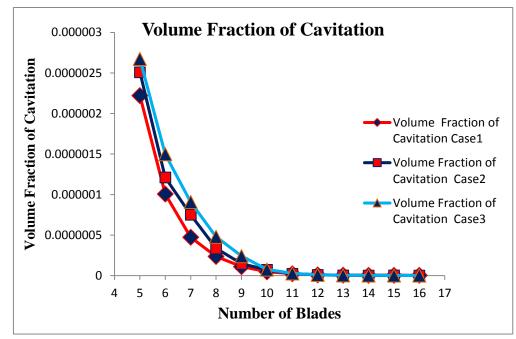**Figure 6** . Pump Efficiency.

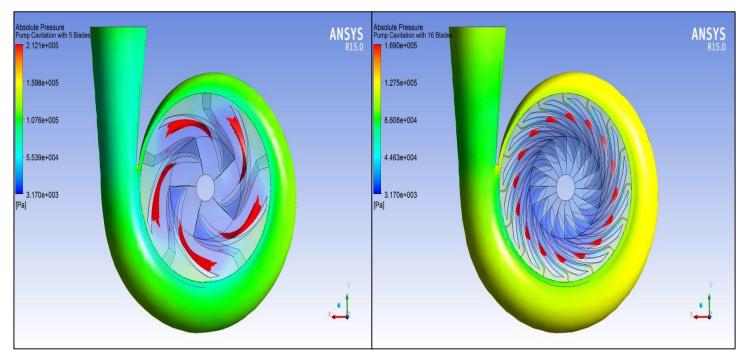**Figure 7** . Volume Fraction of Cavitation.

Figure 8. Comparison of cavitation regions at 5 and 16 number of blades in case1.
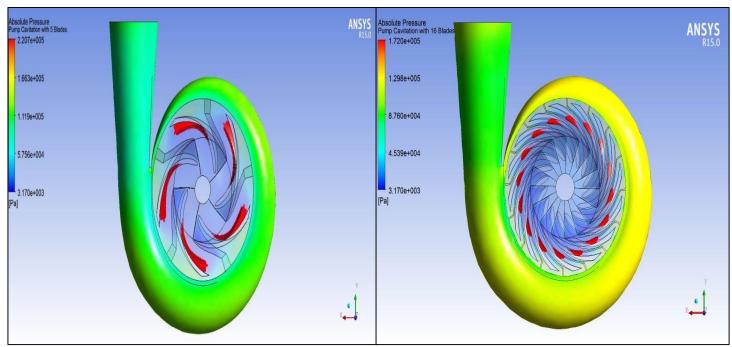
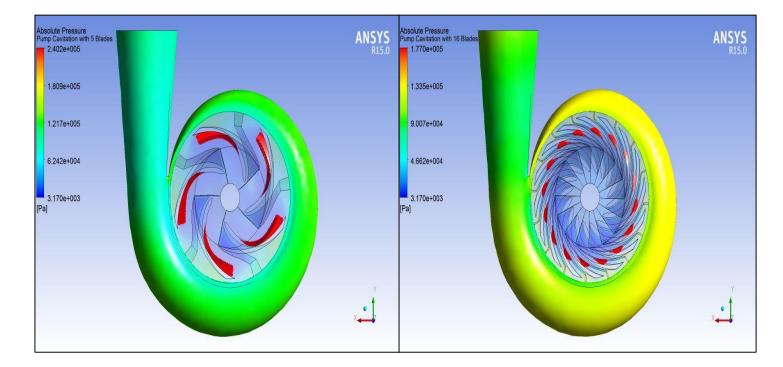**Figure 9.** Comparison of cavitation regions at 5 and 16 number of blades in case2.

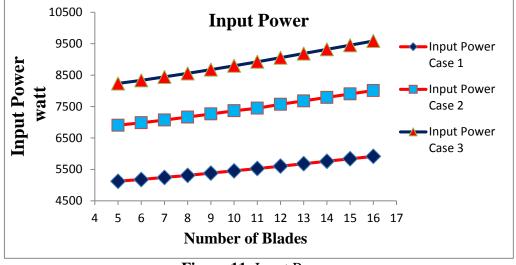**Figure 10.** Comparison of cavitation regions at 5 and 16 number of blades in case3**.**

Figure 11. Input Power.

5. CONCLUSION

Commercial CFD software was applied to analyze water flow attitude through a centrifugal pump, and to study pump performance and cavitation prediction with variation of blade numbers. The method is based on fixing parameters of the centrifugal pump which are volume flow rate, rotating speed, outlet diameter, flow coefficient, and capacity coefficient. The simulation was performed by using turbulence model Shear Stress Transport (SST). The results explain that increment of blade numbers has a significant effect on minimizing pump cavitation, as well as improving pump performance.

Figures and analysis in this study reveal effects of the variation of blade numbers on pump performance and cavitation prediction, it is probable to conclude that: Pump performance can be improved by increasing number of blades. Moreover, Cavitation can be minimized with this increment. However, this optimization has a disadvantage which is increasing electrical consumption. Thus, the results and methods of the study can be important and useful for centrifugal pump design.

6. REFERENCES

1- Coulson, J.M. and Richardson, J.F., "Coulson & Richardson's Chemical Engineering", Volume 1, Fluid Flow, Heat Transfer and Mass Transfer, 6 Ed. Butter worth –Heinemann, 1999.

2- Wright, T.,"Fluid Machinery Performance, Analysis, and Design", USA, CRC press, 1999.

3- Cengel, Y.A. and Cimbala, M. J., "Fluid Mechanics Fundamental and Applications", 1st Ed. New York, McGraw-Hill, 2006.

4- Darby, R.," Chemical Engineering Fluid Mechanics", 2nd Ed. New York, Marcel Dekker, 2001.

5- Katz, J., "Introductory Fluid Mechanics", 1st Ed. New York, Cambridge University Press, 2010.

6- Bar-Meir, G., "Basics of Fluid Mechanics", last modified: Version 0.3.4.0 March 17, 2013, www.potto.org/downloads.php.

7- Crowe, C.T., Elger, D.F., Williams, C.B. and Roberson, J.A.," Engineering Fluid Mechanics", 9 Ed. John Wiley and Sons, Inc., 2009.

8- Gopalakrishman, S., "Modern Cavitation Criteria for Centrifugal Pump", Proceeding of the Second International Pump Symposium, pp. 3-10.

9- Abbas, M.K.," Cavitation in Centrifugal Pump", Diyala Journal of Engineering Sciences, First Engineering Scientific Conference College of Engineering –University of Diyala 22-23 December. 2010, pp. 170-180.

10- Marathe, S.P., Saxena, R. R. and Solanki, C. H. "Numerical Analysis on the Performance Characteristics of the Centrifugal Pump", International Journal of Engineering Research and Applications, vol. 3, Issue 3, 2013, pp.1466-1469.

11- Hassan, A. A. and Kamal, N. A., "Experimental and Numerical Study on Cavitation Effects in Centrifugal Pumps", Journal of Engineering, Vo. 20, No. 2, 2014, pp.73-86.

12- Somashekar, D., Purushothama, H. R., "Numerical Simulation of Cavitation Inception on Radial Flow Pump" , Journal of Mechanical and Civil Engineering, Vo.1, Issue 5 ,2012, PP. 21-26.

13- Jensen, J. and Dayton, K. "Detecting Cavitation in Centrifugal Pumps Experimental Results of the Pump Laboratory", Research and Development, 2000, pp. 26-30.

14- Wee, C. K., Unsteady Flow in Centrifugal Pump at Design and off-Design Conditions, doctoral diss., National University, Singapore, 2011.

15- Ansys, ANSYS Turbo System User's Guide, ANSYS$^{®}$ Blade Modeler™ Release 15.0. United States, Software handbook, November, 2013, 147-180.

16- Brennen, C. E., Hydrodynamics of pumps (Cambridge University Press, 2011).

17- Shah, S. R., Jain, S. V., Patel, R. N. and Lakhera, V. J , "CFD for centrifugal pumps: a review of the state-of-the –art", SciVerse Science Direct, Procedia Engineering 51, 2013, pp. 715 – 720.

18- Cheah, K.W., Lee, T. S. and Winoto, S.H., "Numerical Study of Inlet and Impeller Flow Structures in Centrifugal Pump at Design and off-design Points", International Journal of Fluid Machinery and Systems, Vol. 4, No.1, 2011, pp. 25-32.

19- Li, Wenguang, and Yuliang Zhang. "Numerical simulation of cavitating flow in a centrifugal pump as turbine." Proceedings of the Institution of Mechanical Engineers, Part E: Journal of Process Mechanical Engineering ,2016.

20- Li, Wen-Guang. "Modeling Viscous Oil Cavitating Flow in a Centrifugal Pump." Journal of Fluids Engineering 138.1,2016.

21- Ansys, ANSYS FLUENT Theory Guide, Release 14.0. United States, Software handbook, November, 2011, 491- 616.

22- Sakran, Hayder Kareem. "NUMERICAL ANALYSIS OF THE EFFECT OF THE NUMBERS OF BLADES ON THE CENTRIFUGAL PUMP PERFORMANCE AT CONSTANT PARAMETERS." Technology 6.8 (2015): 105-117.

NOMENCLATURE

C_H　　　Head Coefficient [dimensionless]

C_Q　　　Capacity Coefficient [dimensionless]

D_ω　　　Cross-diffusion of ω [m²/s]

D^+_ω　　　Positive portion of the cross-diffusion term [m²/s]

F　　　Body force [N]

g　　　Gravitational acceleration [m/s²]

k　　　Turbulent kinetic energy [m²/s²]

$\dot{m}_{qp}$　　　Mass transfer from phase q to phase p [kg/s]

$\dot{m}_{pq}$　　　Mass transfer from phase p to phase q [kg/s]

n　　　Number of phases

N_{ss}　　　Suction Specific Speed [dimensionless]

$\dot{Q}$　　　Flow rate capacity [m³/s]

S　　　Modulus of the mean rate-of-strain tensor [s⁻¹]

y　　　Distance to the next surface [m]

V_m　　　Mass-averaged velocity [m/s]

$V_{dr,\,k}$　　　Drift velocity [m/s]

GREEK LETTERS

α Volume fraction [dimensionless]

α^* Damping coefficient for the turbulent viscosity causing a Low-Reynolds number correction [dimensionless]

μ_t Turbulent viscosity [Ns/m^2]

μ_m Viscosity of the mixture [Ns/m^2]

ρ_m Mixture density [kg/m^3]

σ_k Turbulent Prandtl numbers for k [dimensionless]

σ_ω Turbulent Prandtl numbers for ω [dimensionless]

ω Specific dissipation rate [1/s]

ω Pump shaft rotational speed [radian/s]